

See discussions, stats, and author profiles for this publication at: <http://www.researchgate.net/publication/47642945>

A mathematical model for describing the mechanical behaviour of root canal instruments

ARTICLE *in* INTERNATIONAL ENDODONTIC JOURNAL · OCTOBER 2010

Impact Factor: 2.97 · DOI: 10.1111/j.1365-2591.2010.01801.x · Source: PubMed

CITATIONS

9

READS

32

3 AUTHORS, INCLUDING:



[Gary Shun Pan Cheung](#)

The University of Hong Kong

115 PUBLICATIONS 2,921 CITATIONS

[SEE PROFILE](#)



[Yufeng Zheng](#)

Peking University

392 PUBLICATIONS 6,444 CITATIONS

[SEE PROFILE](#)

A mathematical model for describing the mechanical behaviour of root canal instruments

E. W. Zhang¹, G. S. P. Cheung² & Y. F. Zheng¹

¹Department of Advanced Materials and Nanotechnology, College of Engineering, Peking University, Beijing; and ²Area of Endodontics, Comprehensive Dental Care, Faculty of Dentistry, the University of Hong Kong, Hong Kong Special Administrative Region, China

Abstract

Zhang EW, Cheung GSP, Zheng YF. A mathematical model for describing the mechanical behaviour of root canal instruments. *International Endodontic Journal*, **44**, 72–76, 2011.

Aim The purpose of this study was to establish a general mathematical model for describing the mechanical behaviour of root canal instruments by combining a theoretical analytical approach with a numerical finite-element method.

Method Mathematical formulas representing the longitudinal (taper, helical angle and pitch) and cross-sectional configurations and area, the bending and torsional inertia, the curvature of the boundary point and the (geometry of) loading condition were derived. Torsional and bending stresses and the resultant deformation were expressed mathematically as a function of these geometric parameters, modulus of elasticity of the material and the applied load. As illustrations, three brands of NiTi endodontic files of

different cross-sectional configurations (ProTaper, Hero 642, and Mani NRT) were analysed under pure torsion and pure bending situation by entering the model into a finite-element analysis package (ANSYS).

Results Numerical results confirmed that mathematical models were a feasible method to analyse the mechanical properties and predict the stress and deformation for root canal instruments during root canal preparation.

Conclusions Mathematical and numerical model can be a suitable way to examine mechanical behaviours as a criterion of the instrument design and to predict the stress and strain experienced by the endodontic instruments during root canal preparation.

Keywords: bending, finite-element analysis, mechanical property, nickel–titanium, root canal instrument, torsion.

Received 19 June 2010; accepted 26 August 2010

Introduction

Fracture of root canal instruments in use may be as a result of either one or a combination of two reasons: torsional overload and flexural (bending) fatigue (Camps & Pertot 1994). Using a mathematical approach, Turpin *et al.* (2000) studied the influence of two cross-sectional configurations on the torsional and bending stresses in root canal instruments using a boundary integral method. However, it seemed to

appear that their calculations did not fully account for the curvature of the boundary and the area of the cross section. It is also unknown whether a non-linear approach was used. A finite-element method was employed by Berutti *et al.* (2003) to examine two brands of NiTi instrument and, later, by Xu & Zheng (2006) for six different brands. Both studies took into account the non-linear mechanical property of the material but, then, only a cylindrical segment of each instrument was modelled and examined; the longitudinal configuration was not accounted for or included. Thus, the aim of this study was to develop a comprehensive mathematical model that takes into account both the geometrical parameters and the loading conditions (both torsion and bending) for NiTi root

Correspondence: Professor Yu-Feng Zheng, Department of Advanced Materials and Nanotechnology, College of Engineering, Peking University, Beijing 100871, China (Tel. & Fax: +86 10 6276 7411; e-mail: yfzheng@pku.edu.cn).

canal instruments with a non-linear mechanical behaviour.

Geometry of the file design

Figure 1 depicts the longitudinal geometry of an endodontic file. The origin of reference coordinate (on the X-Y plane) runs along the centroid of the cross section (i.e. the z-axis) with radius of the outermost circumcircle at the tip = R_0 ; z represents the distance from the tip to a certain length along the axis of the instrument, which is an independent variable. The maximum radius (R) of a particular cross section is a function of z and the taper $T(z)$ such that

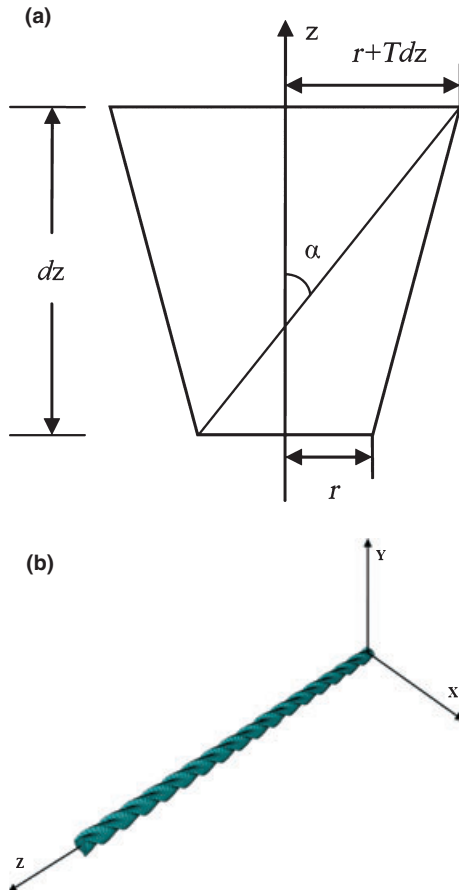


Figure 1 (a) Schematic drawing depicting the geometric parameters for a small section, thickness = dz , of a root canal instrument (tip pointing downward); and (b) example of a 3D finite-element model and the reference coordinate for a 10-mm-long segment of a size 30 Hero 642 instrument with a 0.02 taper.

$$R(z) = R_0 + \frac{1}{2} \int_0^z T(z) dz \quad (1)$$

The relative angle (β) for the orientation of the cross section between two planes, distance dz apart (Fig. 1-a,b), may be expressed as:

$$\beta(z) = \int_0^z \frac{\tan(\alpha(z))}{R(z)} dz \quad (2)$$

and,

$$\beta(z + \lambda(z)) - \beta(z) = 2\pi/k \quad (3)$$

where $\lambda(z)$ is the screw-pitch of the cutting edge, and k is a constant number that is related to the polar symmetry of the cross section. For example, $k = 3$ for HERO (Micro-Mega, Besançon, France) or ProTaper instrument (Dentsply Maillefer, Ballaigues, Switzerland) with a symmetry of 120° , $k = 2$ for NRT (Mani, Tokyo, Japan) with a symmetry of 180° .

When $T(z)$ and $\alpha(z)$ are constant, i.e. for instruments with regular body taper, Eqns (1–3) can be rewritten as:

$$\left. \begin{aligned} R(z) &= R_0 + \frac{1}{2} Tz \\ \beta(z) &= \frac{2 \tan(\alpha)}{T} \ln(1 + \frac{T}{2R_0} z) \\ \lambda(z) &= (e^{\frac{\pi T}{k \tan(\alpha)}} - 1)z + \frac{2R_0}{T} (e^{\frac{\pi T}{k \tan(\alpha)}} - 1) \end{aligned} \right\} \quad (4)$$

Meanwhile, all parameters of the cross section vary with the coordinate z , the cross-sectional parameters such as area (A), torsional inertia (I_t) and bending inertia (I_b) can be written as a function of z in the following formulas:

$$A = \int_{A(z)} dA, \quad I_t = \int_{A(z)} r^2 dA, \quad I_b = \int_{A(z)} h^2 dA \quad (5)$$

where $A(z)$ is the integral area of the cross section at distance z from the tip; r is the distance between the integral point to the centre of the cross section at the coordinate z ; and h is the distance from the integral point to the bending neutral plane.

Equation (5) cannot be calculated analytically because of the complicated boundary around the cross section (Low *et al.* 2006). However, these equations are useful for establishing a finite-element numerical model for defining the torsional and bending parameters of the instrument under torsion and/or bending.

Torsional consideration

When a pure torsional moment is applied to the instrument, the stress τ at any given point on a particular cross-sectional plane can be expressed as follows (Boresi *et al.* 1993):

$$\tau = \frac{M_t}{I_t} \frac{Ae^{|K-\frac{1}{r_m}|}}{\pi r_m^2} r \quad (6)$$

where

M_t : Torsional moment of force (torque)

I_t : Polar moment of inertia

r : Distance from the point under consideration to the centroid of the cross section

r_m : Maximum radius in the direction of r

A : Area of the cross section

K : The curvature of boundary point in the direction of r . Its value can be represented by a piecewise function: when boundary is concave, $K = -1/r$ (the latter being curvature radius); when boundary is a straight line, $K = 0$; when boundary is convex, $K = 1/r$. For any given point, $K = (K_a + K_b)/2$, where K_a and K_b are the curvatures of right and left neighbour points of that location, respectively.

To simplify Eqn (6), V can be defined as a constant that includes all the dimensional variables of the cross section, such that

$$f = \frac{Ae^{|K-\frac{1}{r_m}|}}{\pi r_m^2} \quad (7)$$

This value, which varies with measurements of the cross section (A , r_m and K), may be regarded as a measure of the degree of stress concentration (Boresi et al. 1993). The larger the value of f (because of, say, a small r_m), the greater the stress concentration. In the case of a circular cross section, (with $r_m = r_o$, the latter being the maximum radius of the considered cross section), then $K = 1/r_o$, $A = \pi r_o^2$ and $f = 1$. Then, Eqn (6) can be reduced to:

$$\tau = \frac{M_t}{I_t} r \quad (8)$$

This equation is the well-known formula for pure torsional stress distribution for a cylindrical bar (Boresi et al. 1993). Turpin et al. (2001) used this Eqn (8), but did not consider the influence of the effective radius for a notch (i.e. bottom of a flute) and the curvature of boundary point. Clearly, Eqn (6) would be a more comprehensive formula to describe the mechanical behaviour of the NiTi instrument.

The angle-of-twist (i.e. relative angle between two cross sections as a result of the applied stress) because of the torsional stress is given by:

$$\varphi = \int_{z_1}^{z_2} \frac{M_t}{GI_t} dz = \frac{M_t}{G} \int_{z_1}^{z_2} \frac{dz}{I_t(z)} \quad (9)$$

where the polar moment of inertia $I_t(z) = \int_{A(z)} r^2 dA$, and G is the shear modulus. For an isotropic material, G

is related to its Young's modulus (E) and the Poisson's ratio (ν) such that

$$G = \frac{E}{2(1+\nu)}$$

Bending consideration

Under pure bending, the end-deflection of a regular beam is given by (Boresi et al. 1993):

$$f = \frac{M_b L^2}{2EI_b} \quad (10)$$

where M_b is the bending moment, I_b is the second (bending) moment of inertia, L is the deflected length of beam, and E is the elastic modulus. This Eqn (10) should be modified to take into account the variation in the geometry along the length of the instrument.

$$f = \int_0^L \frac{M_b z}{EI_b(z)} dz \quad (11)$$

The bending stress for a beam with an arbitrary cross section, taking into account the cross-sectional dimensions, may be expressed as:

$$\sigma = \frac{M_b}{I_b} \frac{Ae^{|K-\frac{1}{r_m}|}}{\pi r_m^2} h \quad (12)$$

where h is the distance from the considered point to the neutral plane, with other symbols having the same meaning as in Eqn (6). The deformation of root canal instruments depends on the configuration or curvature of the root canal being prepared. Combining the three Eqns (10–12), the bending stress for the instrument may be expressed as:

$$\sigma = \frac{2Ef}{L^2} \frac{Ae^{|K-\frac{1}{r_m}|}}{\pi r_m^2} h \quad (13)$$

From this Eqn (13), it can be realized that the bending stress distribution depends on the deflected length of instrument (L), elastic modulus of the material (E), dimensional variables of the cross section (V) and the distance from the considered point to the neutral plane (h). Notice that the value of h may differ from radius of the outermost circle (which often is referred as the size of the instrument) for that cross section.

Numerical simulation

Three NiTi root canal instruments: ProTaper (Dentsply Maillefer), HERO 642 (Micro-Mega) and NRT (Mani), each with known a cross-sectional configuration, were

modelled for 3D finite-element analysis, taking into account the mathematical considerations described previously. They were examined for stress distribution under pure torsion (applied torsional moment, $M_t = 1.0 \text{ N}\cdot\text{mm}$) and pure bending situation (bending moment, $M_b = 1.0 \text{ N}\cdot\text{mm}$), with the outside diameter of the instrument $r_o = 0.15 \text{ mm}$ (i.e. ISO size 30).

At an applied torque of $1 \text{ N}\cdot\text{mm}$, the maximum torsional stress at the boundary point (i.e. periphery of the cross section) was 490, 730 and 550 MPa for ProTaper, HERO and NRT, respectively. The maximum stress was situated at the 'bottom' of the flute that was closest to the centroid of the cross section (Fig. 2a). The HERO model had the greatest stress concentration that was localized to a small area (i.e. high stress concentration), whereas ProTaper had a gentle gradient of stresses from the periphery to the centre of its cross section.

On bending, the lowest stress was situated at the neutral plane (blue region in Fig. 2b). The maximum stress recorded for the ProTaper, HERO and NRT instruments were 510, 550 and 530 MPa, respectively. The stress increased in value as the distance increased from the neutral plane, with the maximum stress situated at an area furthest away from that plane – just as the bending formula suggested. There was no distinctive stress concentration present at any sharp points of the cross section (i.e. the cutting edge), both in bending and torsion (Fig. 2).

Discussion

The mechanical properties of the instruments are clearly influenced by their geometrical configurations, which include the cross-sectional shape (which determines the bending and torsional inertia), taper, helical angle and pitch. The boundary of the cross section is another important factor influencing the mechanical properties, in other words, the shorter the radial distance between the periphery (or border) and centroid of the cross section, i.e. the so-called 'core diameter' described by some authors (Harty & Pitt Ford 2004), the greater the reaction stresses developed in the instrument, especially in torsion (see Fig. 2a). This behaviour does not change with the coordinate z .

The symmetry of the stress distribution under torsion coincides well with the symmetry of the cross section; the torsional formulas and numerical simulation results both indicated such symmetry. The maximum Von Mises stress are situated at a site closest to the centre, with the stress distribution being polarly symmetrical in relation to the cross-sectional shape, under torsional load. Symmetry of stress distribution was not observed during bending, because the cross section is not symmetrical about any plane along the instrument's axis. Both the second (bending) and polar (torsional) moments of inertia vary inversely with the forth power of the maximum radius (Boresi *et al.*

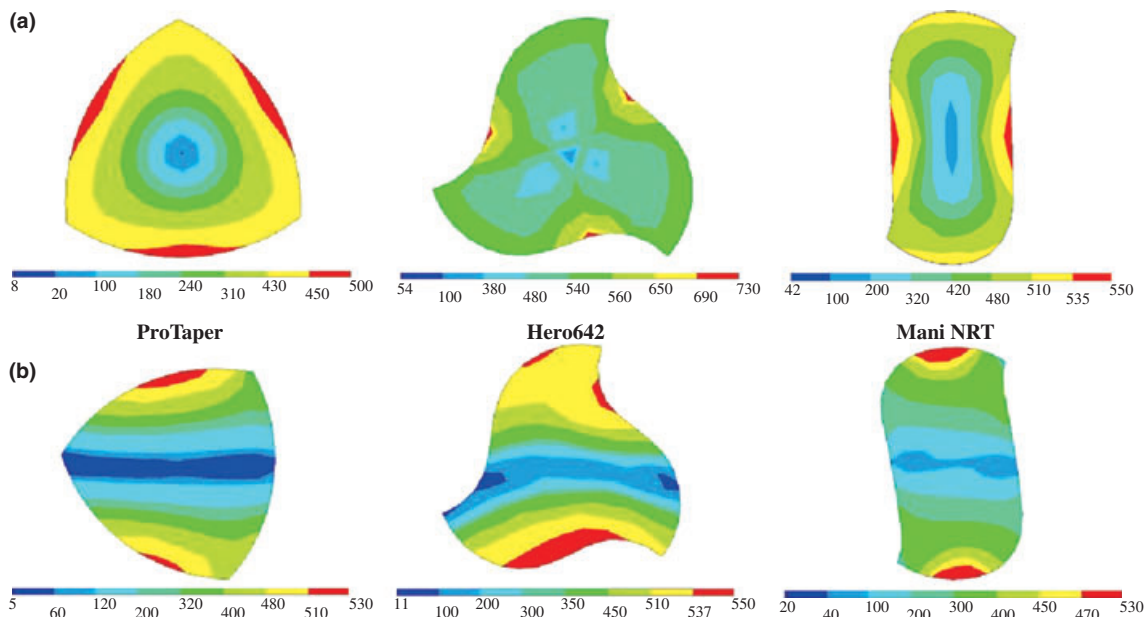


Figure 2 (a) Stress distribution under pure torsion; applied torsional moment $M_t = 1.0 \text{ N}\cdot\text{mm}$. (b) Stress distribution under pure bending; applied bending moment $M_x = 1.0 \text{ N}\cdot\text{mm}$. All the cross sections have the same maximum radius $r_o = 0.15 \text{ mm}$.

1993). Thus, when the radius decreases, the (extent of concentration of) stress increases drastically, in the form of a power function. For the cross-sectional configurations, the bending moment is related to the direction of bending, but the value of bending inertia I_b does not influence the stress directly as in the case of torsion [cf. Eqns (8) and (13)]. The maximum stresses always appear at the periphery (border) of the instrument's cross section, for both torsion and bending loads (Fig. 2). It follows that the cross-sectional configuration of an instrument will affect its apparent strength and susceptibility to fatigue failure.

Other parameters can influence the mechanical properties by modifying the characteristics of the cross section. The maximum radius and the inertia of the cross section along coordinate z would vary for instruments of different tapers. The helical angle (orientation of the flutes) would not alter the radius but changes the orientation of the cross section, so that the bending inertia will change at the same time. The pitch and relative orientation can be calculated for regularly tapered instruments, as they are related to the helical angle and the radius; see Eqns (4) and (5). With all geometrical parameters taken into account, the mechanical behaviour of root canal instruments may then be predicted in a numerical finite-element model. Distribution of (residual) stress and strain can be visualized for various designs of instrument that is working in simulated root canals of different curvatures and torque settings (Kim et al. 2008).

Conclusions

Mathematical and numerical models appear to be a suitable way to examine mechanical behaviour as well as provide a good reference for manufacturers when

designing a new root canal instrument, and for dentists to better understand the limits of the instruments being used for preparing the curved root canals.

References

- Berutti E, Chiandussi G, Gaviglio I, Ibbi A (2003) Comparative analysis of torsional and bending stresses in two mathematical models of nickel-titanium rotary instruments: Pro-Taper versus ProFile. *Journal of Endodontics* **29**, 15–9.
- Boresi AP, Schmidt RJ, Sidebottom ON (1993) *Advanced Mechanics of Materials (Chapter 6 and 16)*, 5th edn. Hoboken, NJ: John Wiley.
- Camps J, Pertot WJ (1994) Torsional and stiffness properties of Canal Master-U stainless-steel and nitinol instruments. *Journal of Endodontics* **20**, 395–8.
- Harty FJ, Pitt Ford TR (2004) *Harty's Endodontics in Clinical Practice*, 5th edn. Edinburgh, UK: Edinburgh Wright.
- Kim HC, Shun PG, Lee CJ, Kim BM, Park JK, Kang SI (2008) Comparison of forces generated during root canal shaping and residual stresses of three nickel-titanium rotary files by using a three-dimensional finite-element analysis. *Journal of Endodontics* **34**, 743–7.
- Low D, Ho AW, Cheung GS, Darvell BW (2006) Mathematical modeling of flexural behavior of rotary nickel-titanium endodontic instruments. *Journal of Endodontics* **32**, 545–8.
- Turpin YL, Chagneau F, Vulcain JM (2000) Impact of two theoretical cross-sections on torsional and bending stresses of nickel-titanium root canal instrument models. *Journal of Endodontics* **26**, 414–7.
- Turpin YL, Chagneau F, Bartier O, Cathelineau G, Vulcain JM (2001) Impact of torsional and bending inertia on root canal instruments. *Journal of Endodontics* **27**, 333–6.
- Xu X, Zheng Y (2006) Comparative study of torsional and bending properties for six models of nickel-titanium root canal instruments with different cross-sections. *Journal of Endodontics* **32**, 372–5.